

Electronic Supporting Information (ESI) For *Dalton Transactions* 2018

Bright Thermal (Blackbody) Emission of Visible Light From LnO_2 ($\text{Ln} = \text{Pr, Tb}$), Photoinduced by NIR 980 nm Laser

C. I. Silva Filho,^{a‡} A. L. Oliveira,^{b‡} S. C. F. Pereira,^b Gilberto F. de Sá,^b L. L. da Luz,^{*b,c} S. Alves Júnior^{*a,b,c}

^a Programa de Pós-Graduação em Ciência dos Materiais, UFPE, Recife-PE 50.740-560, Brazil.

^b Departamento de Química Fundamental, UFPE, Recife-PE 50.740-560, Brazil. E-mail addresses: salvesjr@ufpe.br (S. Alves Júnior), leonisl@yahoo.com.br (L. L. da Luz).

^c Centro de Tecnologias Estratégicas do Nordeste, Campus MCTI Nordeste, Av. Prof. Luiz Freire, nº01, Recife, CEP: 50740-540, PE, Brazil.

Table of content

Equipment descriptions.....	3
Table S1. Estimated black body temperature from the emission spectra of PrO_2 , Pr_6O_{11} , TbO_2 and Tb_4O_7 irradiated with 980 nm CW laser at power density varying from 50 to 160 W cm^{-2}	4
Figure S1. TG analysis (blue line), DTA (red line) and DTG (gray line) of TbO_2 (a) and PrO_2 (b)	5
Figure S2. SEM images of the commercial Pr_6O_{11} and Tb_4O_7 powders.....	6
Figure S3. Rietveld refinement of the x-ray powder diffraction profiles PrO_2 (a), Pr_6O_{11} (b), TbO_2 (c) and Tb_4O_7 (d). The expected reflection positions are displayed using vertical lines. Secondary phases of $\text{Pr}(\text{OH})_3$ (33.7%), Pr_2O_3 (2.6%) (b) and Tb_2O_3 (5.6%) (d) were included in the refinement, and the contributions of the phases to the adjustment are plotted.....	7
Figure S4. Photograph of the PrO_2 , Pr_6O_{11} , TbO_2 and Tb_4O_7 under excitation with 980 nm CW laser at power density ranging from 50 to 160 W cm^{-2}	8
Figure S5. Photoinduced blackbody emission spectra of Pr_6O_{11} (green circle in (a)) and Tb_4O_7 (blue circle in (d)) recorded under 980 CW laser excitation and adjusted power density from 50 to 160 W cm^{-2} . Each spectrum was adjusted according to Planck's law (solid gray lines) to obtain the blackbody temperature.....	9
Figure S6. Corrected (symbol) and uncorrected (black, green and blues solid line) blackbody spectra of PrO_2 (a), TbO_2 (b) under vacuum recorded with a 980 CW laser excitation and tungsten lamp. The red lines are the planckian curves. The structure in the spectra of the TbO_2 is correlated to melting of the sample and their possible	10

evaporation.....	11
Figure S7. Corrected (b and d) and uncorrected (a and c) blackbody spectra of PrO_2 , TbO_2 under vacuum (40 mPa) and atmospheric conditions. The red lines are the planckian curves. The structure in the spectra of the TbO_2 under vacuum is correlated to melting of the sample and their possible evaporation.....	11
Figure S8. Micrographs of MEV of the synthesized LnO_2 after exposure to 980 laser beam with power density varying from 50 to 160 W cm^{-2} . The smaller scale bar correspond to 200 μm and the largest scale bar correspond to 50 μm	12
Figure S9. X-ray diffraction of LnO_2 powders as synthesized and after exposure to 980 CW laser with power density of 160 W cm^{-2}	13
Figure S10. Double-log plots of pump power vs. integrated intensity of the photoinduced blackbody emission of Pr_6O_{11} (a) and Tb_4O_7 (b) powders under atmospheric pressure.....	14

Equipment descriptions

Powder X-ray diffraction was measured at Bruker D8 Advanced X-ray Diffractometer operating under $\text{CuK}\alpha$ radiation (40 kV, 40 mA) equipped with a LynxEye detector. The diffraction pattern was collected in the 2θ range of 10-70° with a step size of 0.02° and a count time of 1 s per step.

Thermogravimetry-differential thermal analysis (TG-DTA) curves were acquired through a SHIMADZU DTG-60H instrument in the range from 30°C to 1000°C using a platinum crucible, under dynamic synthetic air atmosphere (100 $\text{ml}\cdot\text{min}^{-1}$) and with a heating rate of 10° C. $\cdot\text{min}^{-1}$. The diffuse reflection spectra were obtained through a UV-visible recording spectrophotometer (SHIMADZU, UV-2600, Co., Japan), using BaSO_4 as reference and the optical absorptions were converted from the reflection spectra according to Kubelka-Munk equation.

The photoluminescence properties were performed in a spectrofluorimeter Horiba-Jobin Yvon Fluorolog-3 with double-grating monochromator in the UV-VIS (ultraviolet-visible) emission position, R928P Hamamatsu photomultipliers. All emission spectra were corrected by typical correction spectra provided by the manufacturer. The excitation was performed by coupling a 980 nm continuous diode laser from DMC LTDA. The optical fiber used is a UV/SR fiber from Ocean Optics, with core diameter of 600 μm and length of 1 m. The morphologic structure of oxides was performed using a scanning electron microscopy (SEM) microscope TESCAN MIRA 3 operating at 10 kV. The dynamic light scattering (DLS) analysis were performed from an ethanolic suspension of REOs in a NanoBrook Omni equipment. The temperature of the samples during IR laser excitation was recorded with an IR thermal camera (FLIR T450sc). This camera is equipped with an uncooled Vanadioum Oxide (VoX) microbolometer detector that produces thermal images of 320 x 240 Pixels. Thermal Sensitivity of <0.03°C (30mK). All the measurements were performed at room temperature.

Table S1. Estimated black body temperature from the emission spectra of PrO_2 , Pr_6O_{11} , TbO_2 and Tb_4O_7 irradiated with 980 nm CW laser at power density varying from 50 to 160 W cm^{-2} .

Material	Power density (W cm^{-2})	Temperature (K)
PrO_2	50	487
	60	648
	70	875
	80	1005
	90	1121
	100	1173
	110	1232
	120	1271
	130	1322
	140	1363
	150	1390
	160	1420
Pr_6O_{11}	50	475
	60	589
	70	810
	80	1006
	90	1092
	100	1171
	110	1216
	120	1270
	130	1318
	140	1354
	150	1384
	160	1401
TbO_2	50	462
	60	632
	70	819
	80	993
	90	1100
	100	1154
	110	1196
	120	1261
	130	1298
	140	1327
	150	1352
	160	1383
Tb_4O_7	50	534
	60	738
	70	974
	80	1104
	90	1158
	100	1219
	110	1270
	120	1322
	130	1370
	140	1404
	150	1434
	160	1501

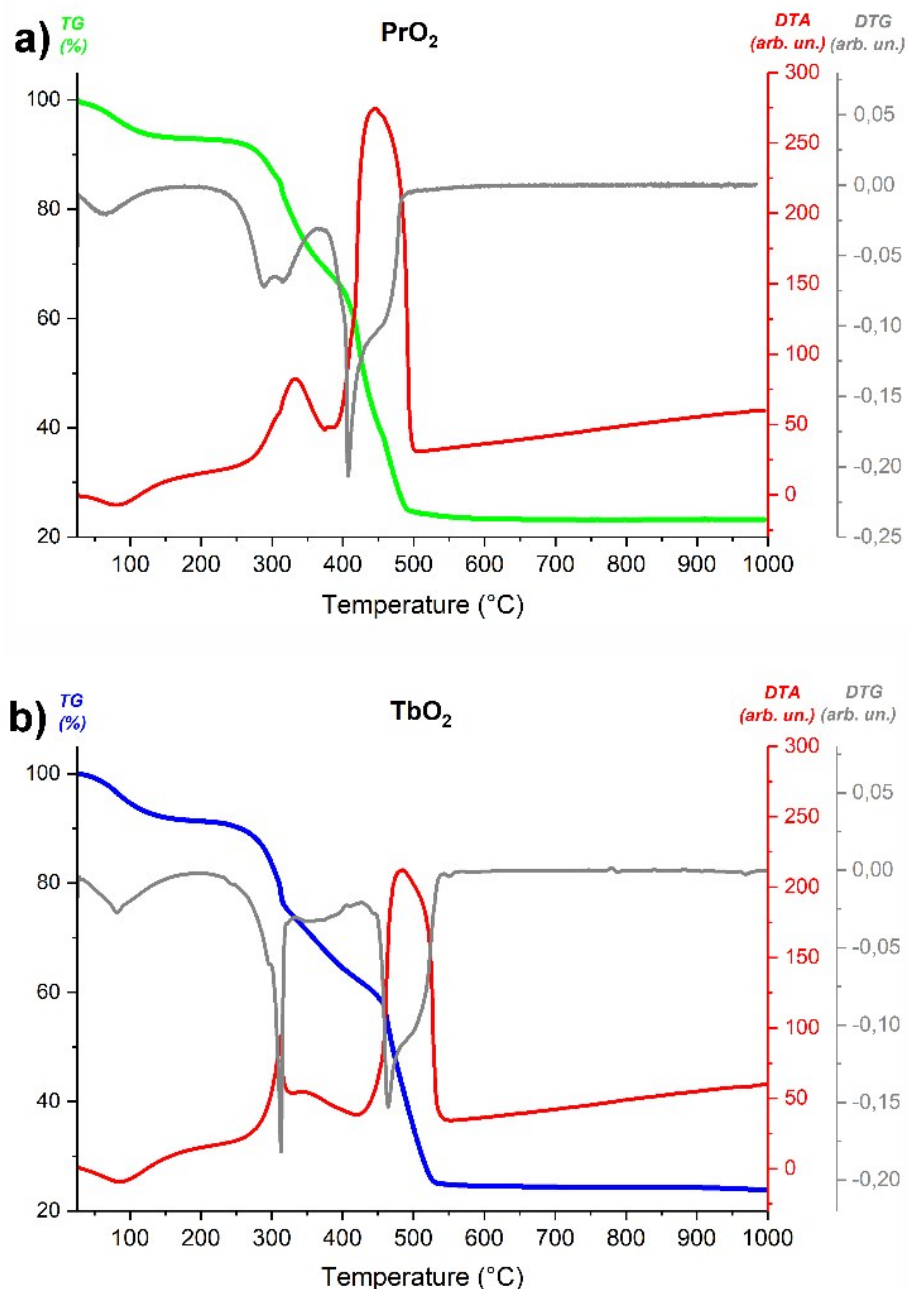


Figure S1. TG analysis (blue line), DTA (red line) and DTG (gray line) of precursors of the TbO_2 (a) and PrO_2 (b) treated at 300 $^{\circ}\text{C}$.

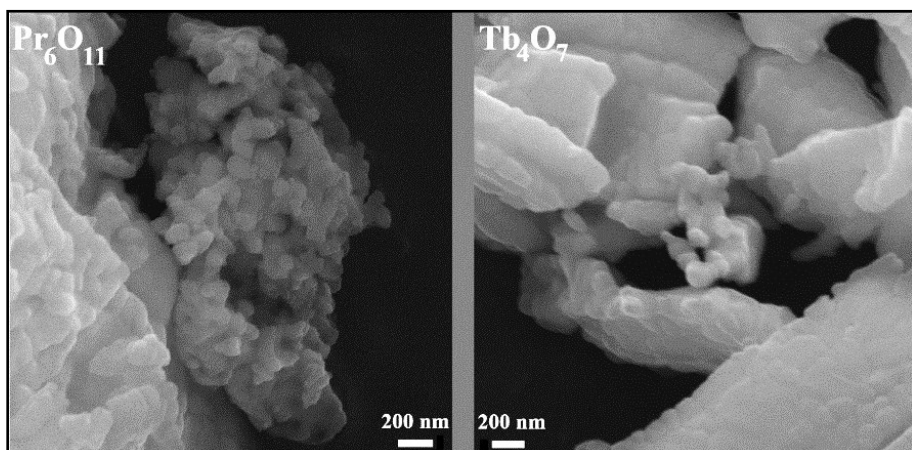


Figure S2. SEM images of the commercial Pr_6O_{11} and Tb_4O_7 powders.

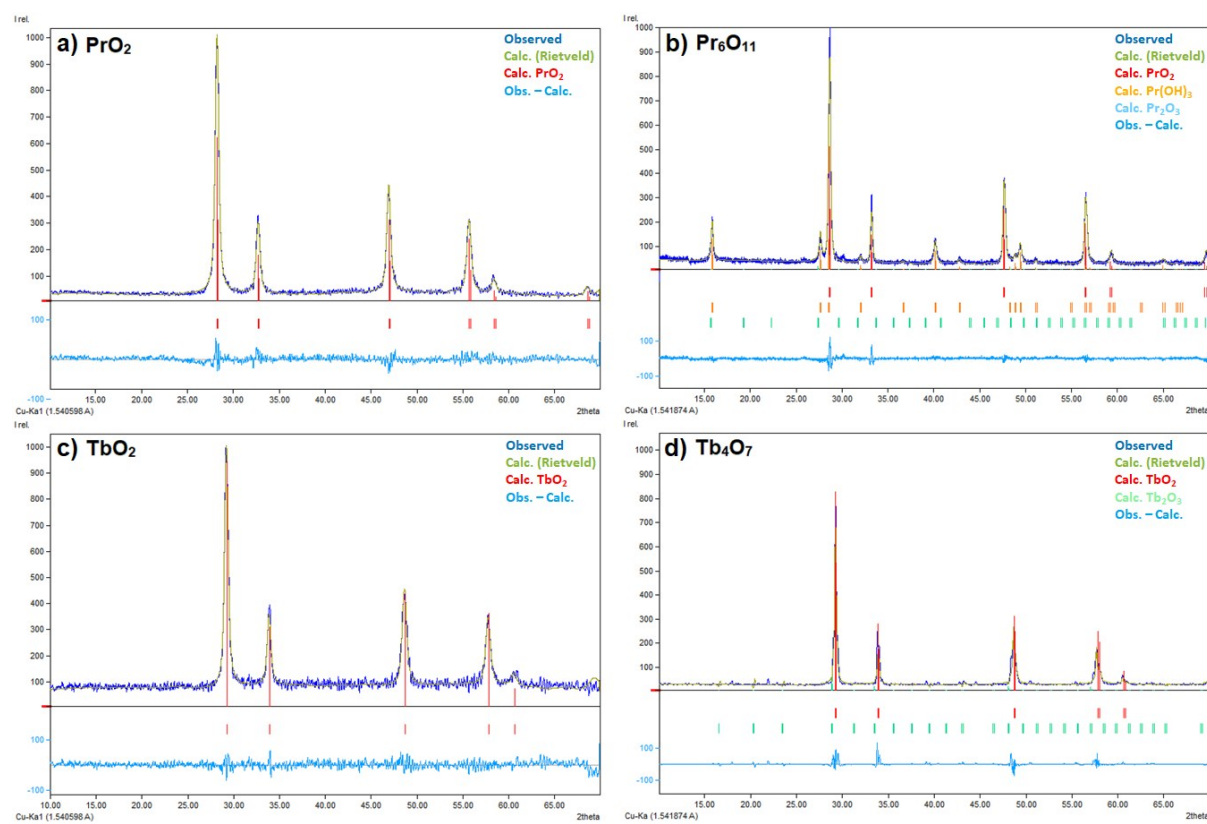


Figure S3. Rietveld refinement of the x-ray powder diffraction profiles PrO_2 (a), Pr_6O_{11} (b), TbO_2 (c) and Tb_4O_7 (d). The expected reflection positions are displayed using vertical lines. Secondary phases of $\text{Pr}(\text{OH})_3$ (33.7%), Pr_2O_3 (2.6%) (b) and Tb_2O_3 (5.6%) (d) were included in the refinement, and the contributions of the phases to the adjustment are plotted.

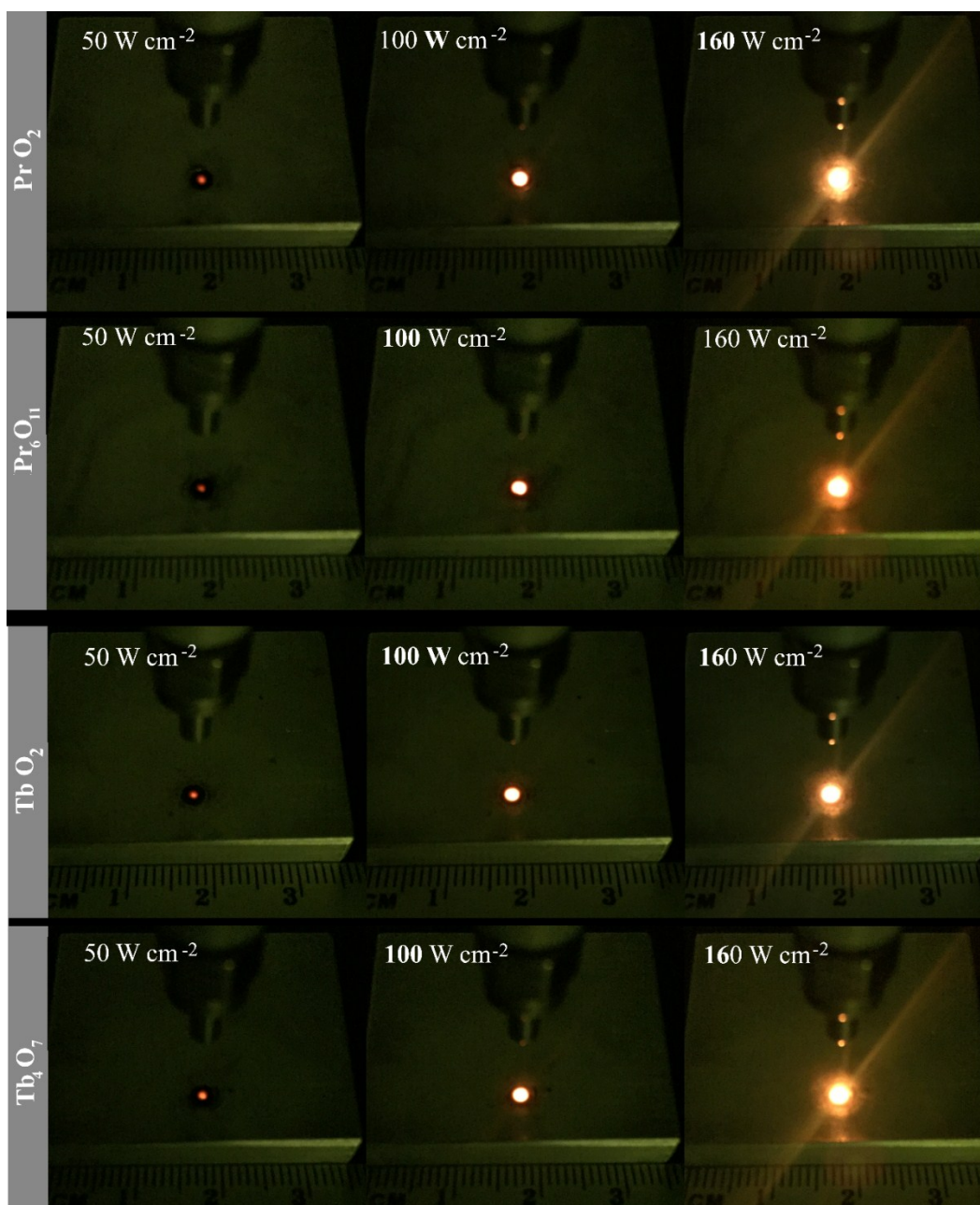


Figure S4. Photograph of the PrO_2 , Pr_6O_{11} , TbO_2 and Tb_4O_7 under excitation with 980 nm CW laser at power density ranging from 50 to 160 W cm^{-2} .

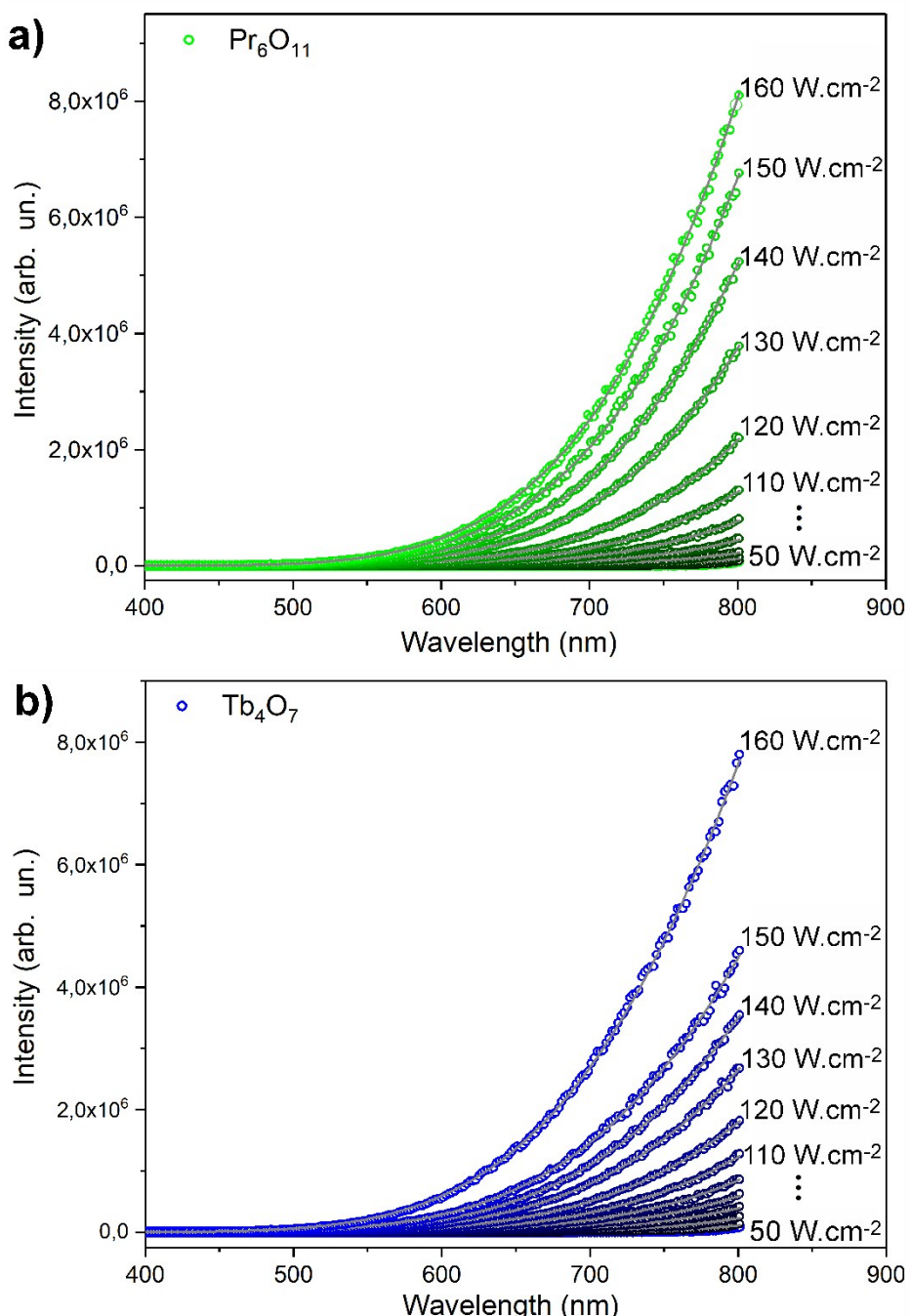


Figure S5. Photoinduced blackbody emission spectra of Pr_6O_{11} (green circle in (a)) and Tb_4O_7 (blue circle in (d)) recorded under 980 CW laser excitation and adjusted power density from 50 to 160 Wcm^{-2} . Each spectrum was adjusted according to Planck's law (solid gray lines) to obtain the blackbody temperature.

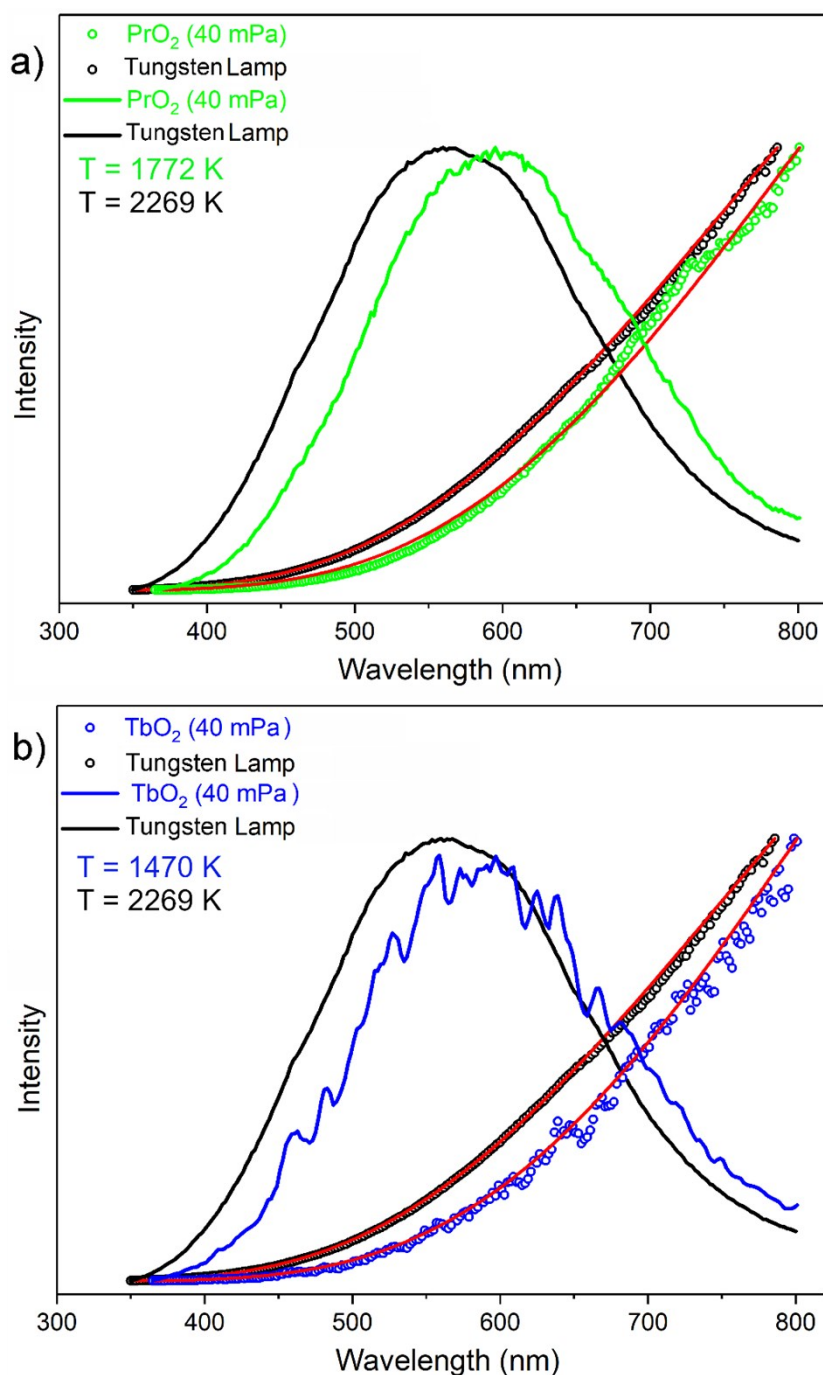


Figure S6. Corrected (symbol) and uncorrected (black, green and blues solid line) blackbody spectra of PrO_2 (a), TbO_2 (b) under vacuum recorded with a 980 CW laser excitation and tungsten lamp. The red lines are the planckian curves. The structure in the spectra of the TbO_2 is correlated to melting of the sample and their possible evaporation.

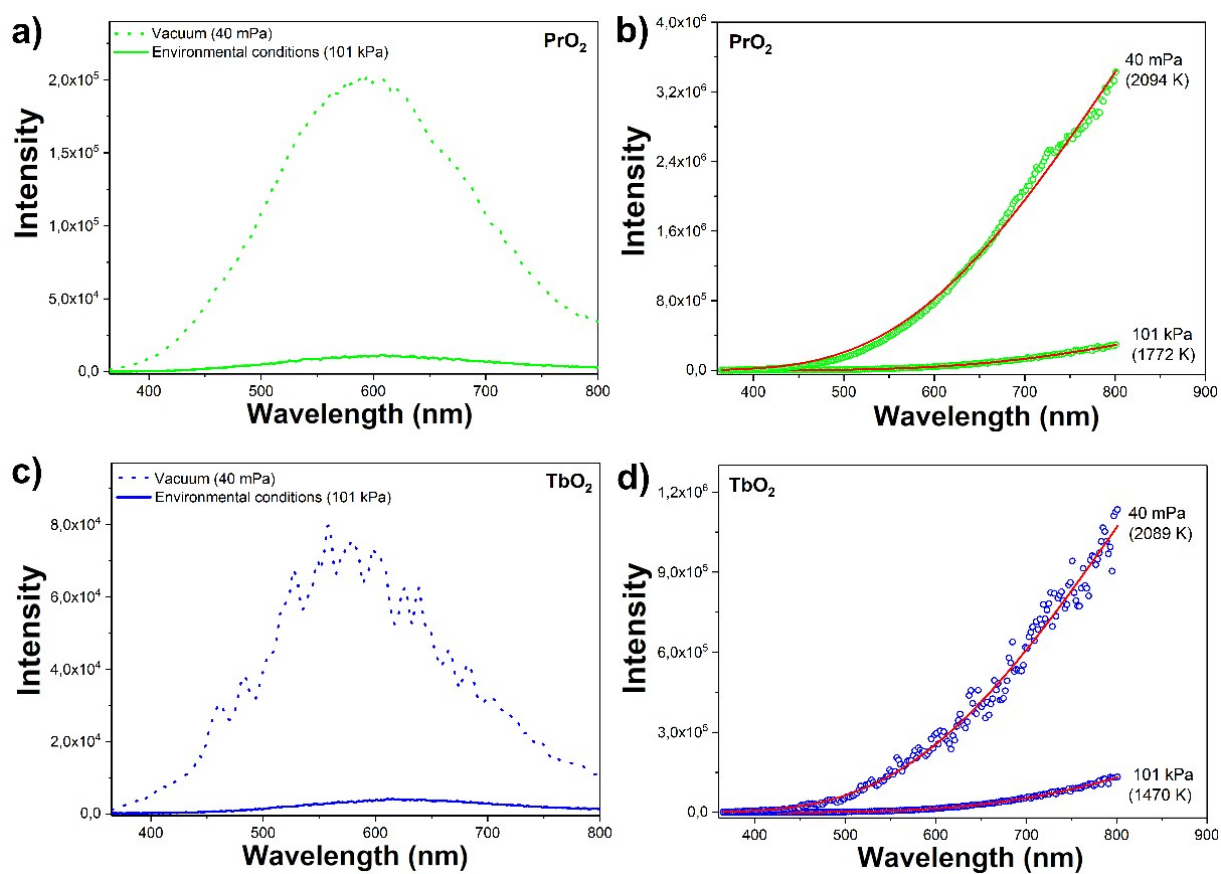


Figure S7. Corrected (b and d) and uncorrected (a and c) blackbody spectra of PrO_2 , TbO_2 under vacuum (40 mPa) and atmospheric conditions. The red lines are the planckian curves. The structure in the spectra of the TbO_2 under vacuum is correlated to melting of the sample and their possible evaporation.

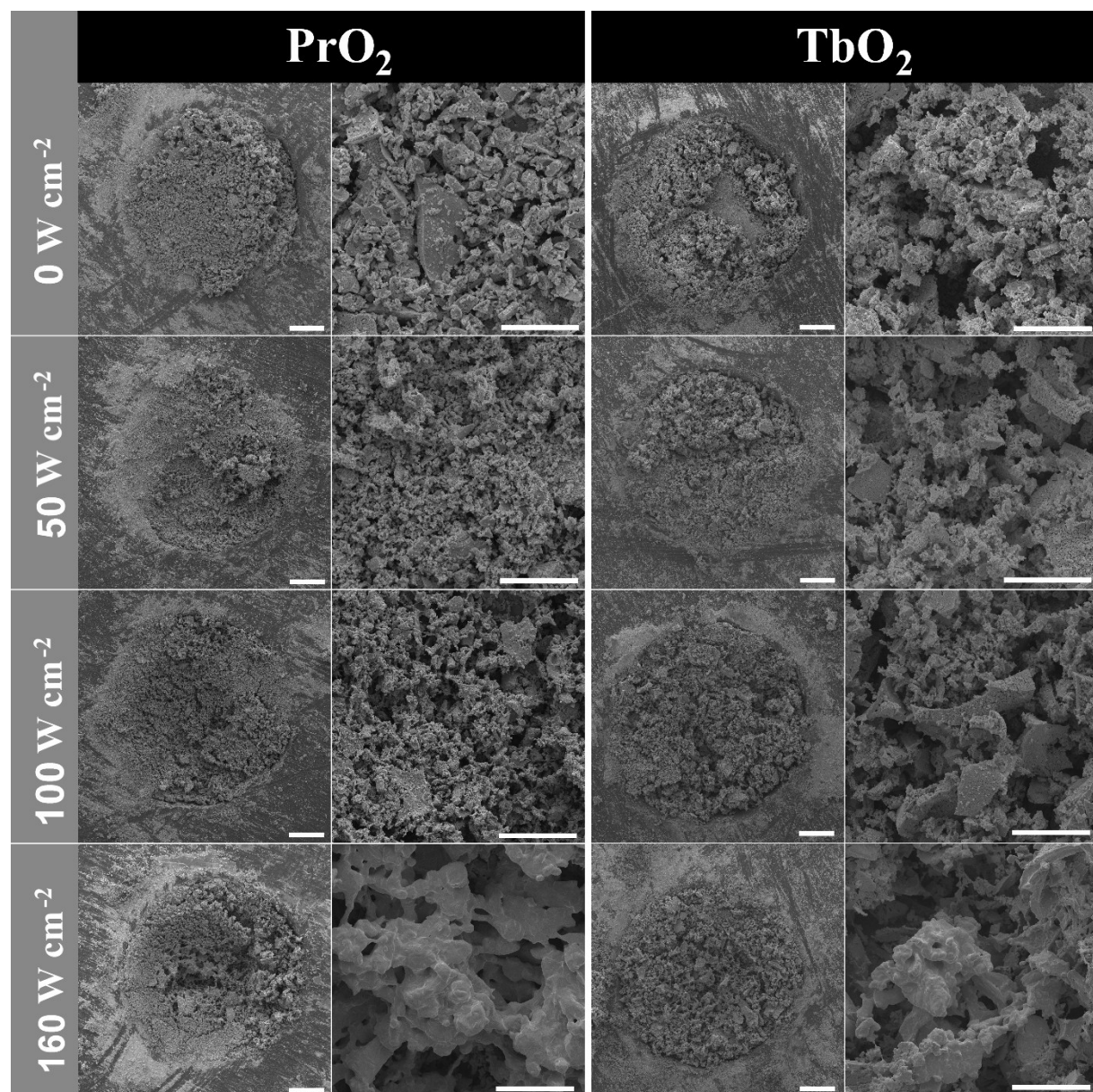


Figure S8. Micrographs of MEV of the synthesized LnO_2 after exposure to 980 laser beam with power density varying from 50 to 160 W cm^{-2} . The smaller scale bar correspond to $200 \mu\text{m}$ and the largest scale bar correspond to $50 \mu\text{m}$.

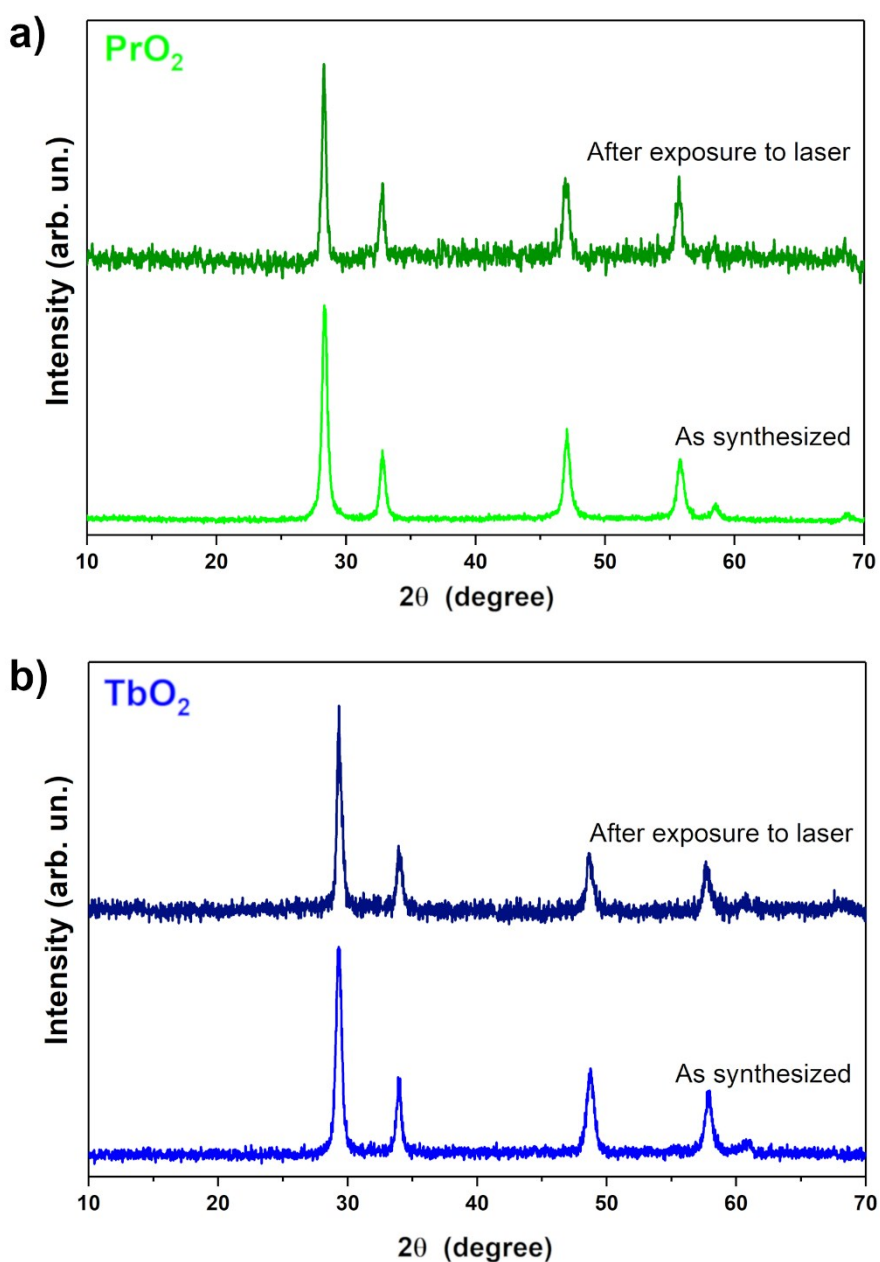


Figure S9. X-ray diffraction of LnO_2 powders as synthesized and after exposure to 980 CW laser with power density of 160 W cm^{-2} .

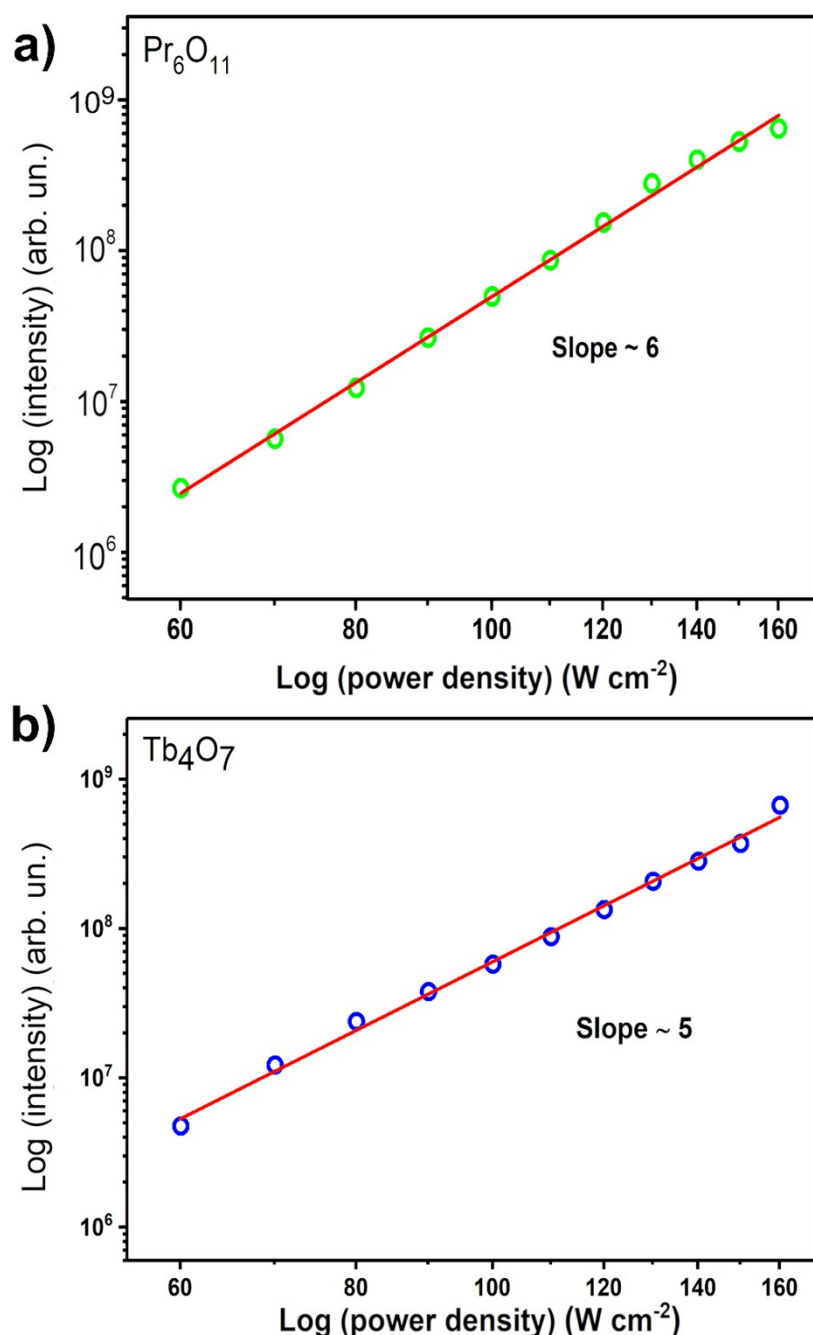


Figure S10. Double-log plots of pump power vs. integrated intensity of the photoinduced blackbody emission of Pr₆O₁₁ (a) and Tb₄O₇ (b) powders under atmospheric pressure.